Enhanced Torque Estimation in Variable Leakage Flux PMSM Combining High and Low Frequency Signal Injection

Diego F. Laborda
University of Oviedo
Dept. of Elect., Computer &
System Engineering
Gijón, Spain
dflaborda@uniovi.es

David Díaz Reigosa
University of Oviedo
Dept. of Elect., Computer &
System Engineering
Gijón, Spain
diazdavid@uniovi.es

Daniel Fernández
University of Oviedo
Dept. of Elect., Computer &
System Engineering
Gijón, Spain
fernandezalodaniel@uniovi.es

Kensuke Sasaki
Nissan Motor Co. Ltd
EV System Laboratory
Atsugi, Kanagawa, Japan
kensuke-sasaki@mail.nissan.co.jp

Takashi Kato
Nissan Motor Co. Ltd
EV System Laboratory
Atsugi, Kanagawa, Japan
katou-t@mail.nissan.co.jp

Fernando Briz
University of Oviedo
Dept. of Elect., Computer &
System Engineering
Gijón, Spain
fernando@isa.uniovi.es

Abstract— Torque measurement/estimation in Variable Leakage Flux Permanent Magnet Synchronous Motors (VLF-PMSMs) is required in many applications. Torque measurement systems are expensive, require extra room, add weight, can introduce resonances into the system and can be sensitive to electromagnetic interference. Alternatively, torque can be estimated, accurate knowledge of machine parameters being often required in this case, which for the case of VLF-PMSMs can be a serious drawback due to the large variation of machine parameters with the operating condition. This paper proposes a torque estimation method for VLF-PMSMs based on stator flux linkage estimation. Machine parameters involved in stator flux linkage estimation are obtained from the response of the machine to a pulsating high frequency current signal and a low frequency and small magnitude, square-wave current signal. Both signals are injected on top of the fundamental excitation and without interfering therefore with the normal operation of the machine.

Keywords— Torque estimation, VLF-PMSMs, variable leakage flux machine, high frequency signal injection, HF signal injection, low frequency signal injection, LF signal injection.

I. INTRODUCTION

Permanent Magnet Synchronous Motors (PMSMs) have been the preferred option for electric and hybrid-electric vehicles (EV & HEV) due to their high torque density, wide speed capability and higher efficiency. Variable flux PMSMs (VF-PMSMs) [1] and variable leakage flux PMSMs (VLF-PMSMs) [2]–[3] have recently been proposed as an alternative to traditional PMSMs in EV & HEV. Their main advantage over traditional PMSMs is that flux-weakening current required in traditional PMSMs to match the back electromotive force with the available voltage in the DC link [4], is highly reduced or even eliminated [1]–[3].

EV & HEV require precise control of the torque produced by the machine [5]–[7], torque measurement/estimation being therefore needed. If torque is to be measured, torque transducers based on strain gauges are likely the preferred option. Less popular alternatives are systems based on torsional displacement methods [8]. Regardless of the method being used, precise torque measurement is expensive, requires room and extra cables, and introduces reliability concerns, torque estimation being therefore preferred [9]–[20]. Torque estimation methods can be roughly classified into torque equation-based methods [9]–[11] and indirect estimation methods [12]–[20]. All these methods [9]–[20] require precise knowledge of machine parameters (resistances, inductances or magnet flux) which can vary with the operating conditions of the machine (e.g. temperature or saturation).

This paper proposes a method to improve the accuracy of torque estimation in VLF-PMSMs. Torque equation requires knowledge of stator flux linkage. Machine parameters needed for stator flux linkage estimation are d and q-axis inductances, stator resistance and permanent magnets (PMs) flux. d and q-axes inductances and stator resistance will be estimated from the response of the machine to a pulsating high frequency (HF) current signal, while the PM flux linkage will be estimated from the response of the machine to a low frequency square-wave current signal. Both signals are low magnitude and are injected on top of the fundamental excitation.

The paper is organized as follows: Section II shows the fundamental model of a VLF-PMSM; Section III presents the proposed torque estimation method; Section IV provides FEA evaluation of the method. Finally, conclusions are provided in Section V.

II. FUNDAMENTAL MODEL OF A VLF-PMSM

The fundamental model of a VLF-PMSM in a reference frame synchronous with the rotor is given by (1) where p stands for the derivative respect to time, R_d, R_q, L_d and L_q are the d and q-axes resistances and inductances respectively, ω_r is the rotor

speed and λ_{pm} is the PM flux linkage; d-axis being aligned with PMs flux. The output torque can be expressed as (2) [21], where P is the number of poles, and λ_{sd}^r and λ_{sq}^r are the stator dq-axis flux linkages, (3) and (4) respectively.

$$\begin{bmatrix} v_{sd}^r \\ v_{sq}^r \end{bmatrix} = \begin{bmatrix} R_d & 0 \\ 0 & R_q \end{bmatrix} \begin{bmatrix} i_{sd}^r \\ i_{sq}^r \end{bmatrix} + p \begin{bmatrix} L_d & 0 \\ 0 & L_q \end{bmatrix} \begin{bmatrix} i_{sd}^r \\ i_{sq}^r \end{bmatrix} +$$
$$+ \begin{bmatrix} 0 & -\omega_r L_q \\ \omega_r L_d & 0 \end{bmatrix} \begin{bmatrix} i_{sd}^r \\ i_{sq}^r \end{bmatrix} + \begin{bmatrix} 0 \\ \lambda_{pm}\omega_r \end{bmatrix} \tag{1}$$

$$T_{out} = \frac{3}{2}\frac{P}{2}\left[\lambda_{sd}^r i_{sq}^r - \lambda_{sq}^r i_{sd}^r \right] \tag{2}$$

$$\lambda_{sd}^r = i_{sd}^r L_d + \lambda_{pm} \tag{3} \qquad \lambda_{sq}^r = i_{sq}^r L_q \tag{4}$$

III. TORQUE ESTIMATION BASED ON FLUX OBSERVER ENHANCED WITH ON-LINE PARAMETERS ESTIMATION

This section presents the proposed torque estimation method based on a flux observer enhanced with on-line parameters estimation. It is observed from (2)-(4) that the output torque of a VLF-PMSM is a function of dq-axes stator flux linkages, which depend on the dq-axes inductances, dq-axes resistances and PM flux [21]. These parameters vary during normal machine operation e.g. due to temperature or saturation. Fig. 2a-d shows the dq-axes inductances, stator resistance and PM flux linkage vs. dq-axes currents of the VLF-PMSMs that will be used for the experimental verification of the proposed method, obtained through FEA. It is observed from this figure that the variation of these parameters with the machine operating condition cannot be ignored, machine parameters estimation being therefore needed. Fig. 1 shows the proposed torque estimation method as well as its integration with machine control.

Torque estimation will require a) stator resistance and inductances estimation, b) stator flux linkage estimation and c) PM flux linkage estimation, this is described in the following sections.
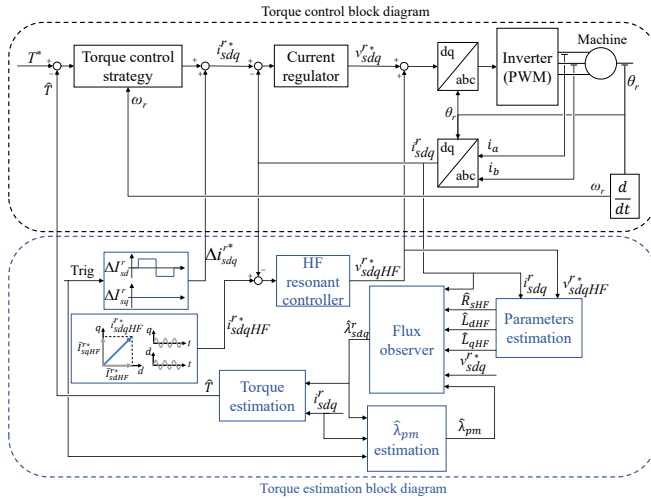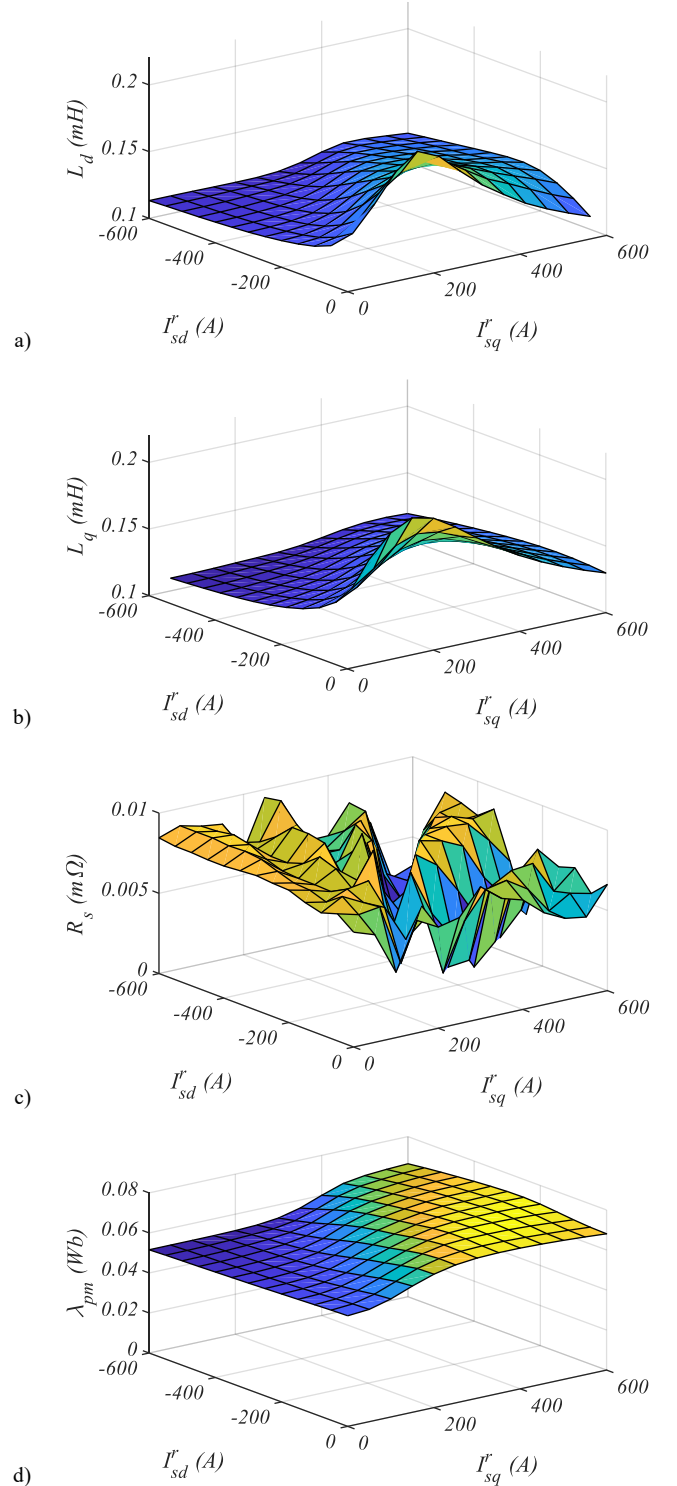
a)

b)

c)

d)

Fig. 2 – a) d-axis inductance vs. stator current, b) q-axis inductance vs. stator current, c) stator resistance vs. stator current and d) PM flux linkage vs. stator current. I_{HF}=0.05 pu, ω_{HF}=2*π*500 rad/s, ΔI_{sd}=0.02 pu, ω_r=500 rpm and T_r=20ºC.

Fig. 1 – Integration of torque estimation and torque control.

A. Resistance and inductances estimation using high frequency signal injection

Injection of a high frequency signal has been shown to be a reliable method for resistance and inductance estimation [11],[22],[23]. In this paper, the injection of a pulsating high frequency current will be used to estimate stator resistance and inductances needed by the flux observer. The method has some similarities with the proposal in [11]. However, the method in [11] required two pulsating HF currents while only one HF signal is required in the method proposed in this paper. This reduces the adverse effects of the HF signal and simplifies the implementation.

If the PMSM is fed with a HF voltage/current, the magnet flux dependent term in (1) can be safely neglected, as it does not contain any HF component, the HF model shown in (5) is obtained, where R_{dHF}, R_{qHF}, L_{dHF} and L_{qHF} are the d and q-axes high frequency resistances and inductances, respectively; i_{sdHF}^r and i_{sqHF}^r are the d and q-axes high frequency currents; v_{sdHF}^r and v_{sqHF}^r are the d and q-axes high frequency voltages; d and q-axis HF inductances and resistances can be obtained by injecting a pulsating HF at 45º from the d axis, (6) of magnitude I_{HF}^* and frequency ω_{HF} (see Fig. 1). A resonant controller can be used for this purpose [11]. The HF voltages that will be commanded by the resonant controller will be of the form shown in (7).

$$\begin{bmatrix} v_{sdHF}^r \\ v_{sqHF}^r \end{bmatrix} = \begin{bmatrix} R_{dHF} & 0 \\ 0 & R_{qHF} \end{bmatrix} \begin{bmatrix} i_{sdHF}^r \\ i_{sqHF}^r \end{bmatrix} + p \begin{bmatrix} L_{dHF} & 0 \\ 0 & L_{qHF} \end{bmatrix} \begin{bmatrix} i_{sdHF}^r \\ i_{sqHF}^r \end{bmatrix} + \\ + \begin{bmatrix} 0 & -\omega_r L_{qHF} \\ \omega_r L_{dHF} & 0 \end{bmatrix} \begin{bmatrix} i_{sdHF}^r \\ i_{sqHF}^r \end{bmatrix} \tag{5}$$

$$i_{sdqHF}^{r*} = \begin{bmatrix} \bar{I}_{sdHF}^{r*} \\ \bar{I}_{sqHF}^{r*} \end{bmatrix} = \begin{bmatrix} I_{HF}^* \cos(\omega_{HF}t) \\ I_{HF}^* \cos(\omega_{HF}t) \end{bmatrix} \tag{6}$$

$$v_{sdqHF}^{r*} = \begin{bmatrix} \bar{V}_{sdHF}^{r*} \\ \bar{V}_{sqHF}^{r*} \end{bmatrix} = \begin{bmatrix} (R_{dHF} + j\omega_{HF}L_{dHF})\bar{I}_{sdHF}^r - \omega_r L_{qHF}\bar{I}_{sqHF}^r \\ (R_{qHF} + j\omega_{HF}L_{qHF})\bar{I}_{sqHF}^r + \omega_r L_{dHF}\bar{I}_{sdHF}^r \end{bmatrix} \tag{7}$$

L_{dHF} can be estimated from the measured d-axis HF current, $i_{sdqHF}^{r'}$ (8), and the commanded d-axis HF voltage, $v_{sdqHF}^{r'}$ (9). Both (8) and (9) can be separated into positive sequence ($i_{sdqHFpc}^{r'}$ and $v_{sdqHFpc}^{r'}$) and negative sequence ($i_{sdqHFnc}^{r'}$ and $v_{sdqHFnc}^{r'}$) components, (10) and (11). The d-axis HF impedance, (12) can be obtained either from the positive or negative sequence component, the d-axis HF inductance being its imaginary part (13).

$$i_{sdqHF}^{r'} = \begin{bmatrix} \bar{I}_{sdHF}^{r*} \\ 0 \end{bmatrix} = \begin{bmatrix} I_{HF}^* \cos(\omega_{HF}t) \\ 0 \end{bmatrix} \tag{8}$$

$$v_{sdqHF}^{r'} = \begin{bmatrix} \bar{V}_{sdHF}^{r*} \\ 0 \end{bmatrix} = \begin{bmatrix} (R_{dHF} + j\omega_{HF}L_{dHF})\bar{I}_{sdHF}^r - \omega_r L_{qHF}\bar{I}_{sdHF}^r \\ 0 \end{bmatrix} \tag{9}$$

$$i_{sdqHF}^{r'} = \frac{|i_{sdqHF}^{r'}|}{2} e^{j\omega_{HF}t} + \frac{|i_{sdqHF}^{r'}|}{2} e^{-j\omega_{HF}t} = i_{sdqHFpc}^{r'} + i_{sdqHFnc}^{r'} \tag{10}$$

$$v_{sdqHF}^{r'} = \frac{|v_{sdqHF}^{r'}|}{2} e^{j(\omega_{HF}t-\varphi_{Zd})} + \frac{|v_{sdqHF}^{r'}|}{2} e^{j(-\omega_{HF}t+\varphi_{Zd})} = \\ = v_{sdqHFpc}^{r'} + v_{sdqHFnc}^{r'} \tag{11}$$

$$Z_{dHF} = R_{dHF} - \omega_r L_{qHF} + j\omega_{HF}L_{dHF} = \frac{v_{sdqHFpc}^{r'}}{i_{sdqHFpc}^{r'}} = \frac{v_{sdqHFnc}^{r'}}{i_{sdqHFnc}^{r'}} \tag{12}$$

$$L_{dHF} = \Im[Z_{dHF}]/\omega_{HF} \tag{13}$$

L_{qHF} can be estimated from the measured q-axis HF current, $i_{sdqHF}^{r''}$ (14), and the commanded q-axis HF voltage, $v_{sdqHF}^{r''}$ (15), using (16)-(19) similarly as for d-axis HF inductance estimation.

$$i_{sdqHF}^{r''} = \begin{bmatrix} 0 \\ \bar{I}_{sqHF}^{r*} \end{bmatrix} = \begin{bmatrix} 0 \\ I_{HF}^* \cos(\omega_{HF}t) \end{bmatrix} \tag{14}$$

$$v_{sdqHF}^{r''} = \begin{bmatrix} 0 \\ \bar{V}_{sqHF}^{r*} \end{bmatrix} = \begin{bmatrix} 0 \\ (R_{qHF} + j\omega_{HF}L_{qHF})\bar{I}_{sqHF}^r + \omega_r L_{dHF}\bar{I}_{sqHF}^r \end{bmatrix} \tag{15}$$

$$i_{sdqHF}^{r''} = \frac{|i_{sdqHF}^{r''}|}{2} e^{j\omega_{HF}t} + \frac{|i_{sdqHF}^{r''}|}{2} e^{-j\omega_{HF}t} = i_{sdqHFpc}^{r''} + i_{sdqHFnc}^{r''} \tag{16}$$

$$v_{sdqHF}^{r''} = \frac{|v_{sdqHF}^{r''}|}{2} e^{j(\omega_{HF}t-\varphi_{Zq})} + \frac{|v_{sdqHF}^{r''}|}{2} e^{j(-\omega_{HF}t+\varphi_{Zq})} = \\ = v_{sdqHFpc}^{r''} + v_{sdqHFnc}^{r''} \tag{17}$$

$$Z_{qHF} = R_{qHF} + \omega_r L_{dHF} + j\omega_{HF}L_{qHF} = \frac{v_{sdqHFpc}^{r''}}{i_{sdqHFpc}^{r''}} = \frac{v_{sdqHFnc}^{r''}}{i_{sdqHFnc}^{r''}} \tag{18}$$

$$L_{qHF} = \Im[Z_{qHF}]/\omega_{HF} \tag{19}$$

dq-axes HF resistance can be obtained from (20) and (21), the stator HF resistance R_{sHF} (22) being the average of the d and q-axis resistances.

$$R_{dHF} = \Re[Z_{dHF}] + \omega_r L_{qHF} \tag{20}$$

$$R_{qHF} = \Re[Z_{qHF}] - \omega_r L_{dHF} \tag{21}$$

$$R_{sHF} = \frac{R_{dHF} + R_{qHF}}{2} \tag{22}$$

B. Stator flux linkage estimation

Different stator flux observers have been proposed in the literature, the voltage model (23)-(24) and the current model (3)-(4) based being the preferred options [24]–[25]. Gopinath type flux observer was proposed in [25], combining the voltage and current models. The advantages and drawbacks of both models can be seen in Table I.

$$\lambda_{sd}^s(t) = \int (V_{sd}^s(t) - R_s \cdot I_{sd}^s(t)) \cdot dt \tag{23}$$

$$\lambda_{sq}^s(t) = \int (V_{sq}^s(t) - R_s \cdot I_{sq}^s(t)) \cdot dt \tag{24}$$

The current model can be used to estimate stator flux in the whole speed range of the machine but parameters, such as magnet flux linkage and inductances, must be previously known. On the other hand, voltage model can be used to estimate machine flux at high speeds [24], at low speeds it becomes inaccurate due to the diminishing magnitude of the Back-EMF

with speed and it cannot be used at standstill. In addition, as a pure integrator is required to estimate the flux, there is an initial estimation error (integration constant) which needs to be compensated.

Gopinath type flux observers combine voltage at high speed and the current model at low speed including standstill, a PI controller being used to make a smooth transition between models. The controller bandwidth will set the transition frequency from current to voltage model. This type of flux observer provides reliable estimation in the whole speed range of the machine, including standstill, being more sensitive to machine parameters at low speeds.

TABLE I. ADVANTAGES AND DRAWBACKS OF FLUX MODELS

	CURRENT MODEL	VOLTAGE MODEL	GOPINATH
Parameter independency	✘	✘	✘
No initial state error	✔	✘	✔
Estimation in the whole speed range, including standstill	✔	✘	✔

The Gopinath type flux observer shown in Fig. 3 will be used in this paper to estimate the stator flux linkage [25]. Observer parameters are estimated using HF signal injection. PM flux linkage estimation discussed in the next section will be used to further enhance the stator flux linkage estimation.
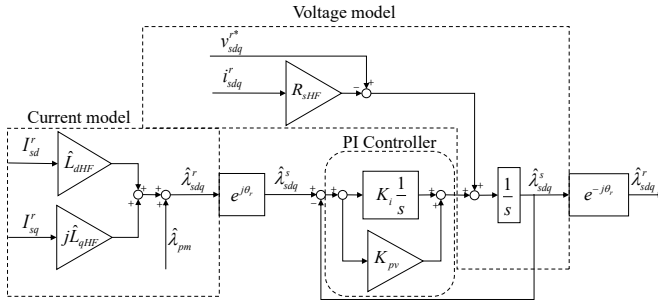

Fig. 3 – Gopinath type flux observer scheme.

C. PM flux linkage estimation

PM flux linkage is relatively easy to estimate from the back-EMF at no load but is difficult to estimate when the machine is loaded. The method proposed in [26] is used, in which λ_{pm} is estimated from the stator flux linkage in combination with the response of the machine to the injection of a quasi-square-wave, small-amplitude and low frequency, current signal (Δi_{sdq}^{r*}). Both signals are injected on top of the fundamental current [26].

The PM flux linkage is estimated from the response of the machine to a low frequency, small magnitude, quasi-square-wave current signal of magnitude ΔI_{sd}^r injected on top of the fundamental current [26], this is schematically represented in Fig. 4. The d-axis stator flux linkage, λ_{sd}^r is represented by (25), λ_{sd}^{r+} is the d-axis flux linkage when positive d-axis current step, ΔI_{sd}^r, is applied (26), while λ_{sd}^{r-} is the d-axis flux linkage when negative d-axis current step, $-\Delta I_{sd}^r$, is applied (27). The stator flux linkages, λ_{sd}^r, λ_{sd}^{r+} and λ_{sd}^{r-} are not obtained using (25)-(27), instead, they are estimated by the Gopinath type flux observer shown in the previous subsection. $\hat{\lambda}_{pm}^+$ and $\hat{\lambda}_{pm}^-$ are

estimated from (28) and (29), respectively. $\hat{\lambda}_{pm}$ (PM flux linkage when no applying ΔI_{sd}^r) is finally obtained as the average of $\hat{\lambda}_{pm}^+$ and $\hat{\lambda}_{pm}^-$, (30).

$$\lambda_{sd}^r = \lambda_{pm} + L_d \cdot I_{sd}^r \tag{25}$$

$$\lambda_{sd}^{r+} = \lambda_{pm}^+ + L_d^+ \cdot (I_{sd}^r + \Delta I_{sd}^r) \tag{26}$$

$$\lambda_{sd}^{r-} = \lambda_{pm}^- + L_d^- \cdot (I_{sd}^r - \Delta I_{sd}^r) \tag{27}$$

$$\hat{\lambda}_{pm}^+ = \frac{1}{\Delta I_{sd}} \left[I_{sd}^r \hat{\lambda}_{sd}^+ - (I_{sd}^r + \Delta I_{sd}^r) \hat{\lambda}_{sd} \right] \tag{28}$$

$$\hat{\lambda}_{pm}^- = \frac{1}{\Delta I_{sd}} \left[(I_{sd}^r - \Delta I_{sd}^r) \hat{\lambda}_{sd}^- - I_{sd}^r \hat{\lambda}_{sd} \right] \tag{29}$$

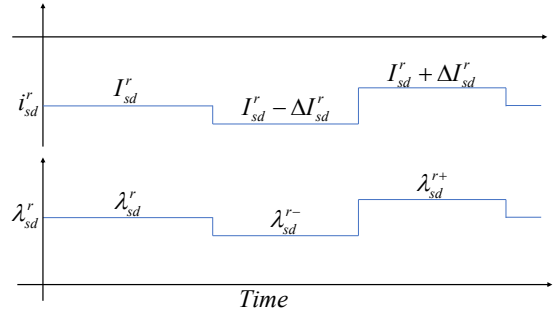$$\hat{\lambda}_{pm} = \frac{\hat{\lambda}_{pm}^+ + \hat{\lambda}_{pm}^-}{2} \tag{30}$$

Fig. 4 – Schematic representation of the injected stator d-axis current, fundamental and small-amplitude, low frequency, squarewave currents, (i_{sd}^r) and resulting stator d-axis flux (λ_{sd}^r).

IV. FEA ANALYSIS OF THE METHOD

Simulation results of the proposed method by means of FEA are provided in this section. Fig. 5 shows the schematic representation of the test machine that will be used for simulation verification. The parameters of the VLF-PMSM test machine are shown in Table II.
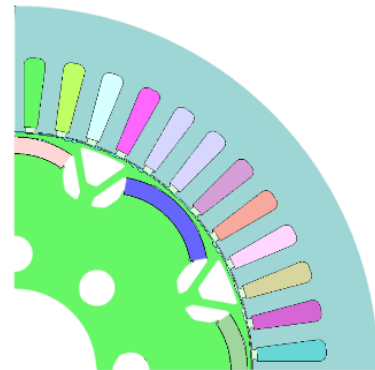

Fig. 5 – Schematic representation of the test machine.

TABLE II. MACHINE PARAMETERS

P_{Rated} [kW]	110
I_{Rated} [A]	640
ω_r [rpm]	10000
T_{Rated} [Nm]	250
Poles	8

Simulations are performed at 500 rpm (low speed) in order to test the proposed method performance in the speed region where the current model dominates the flux observer estimation and the parameter sensitivity is higher. A pulsating HF current signal with $I_{HF} = 0.05$pu is injected to estimate HF inductances and resistance following the method described in Section IV.

A. Cross-coupling inductance effect

The obtained d and q-axes HF inductances are compared with the DC inductances in Fig. 6a and 6b, respectively. The obtained HF and DC values are not matching, this is produced by the relatively high cross-coupling inductance present in VLF-PMSMs. In Section III, the cross-coupling inductance effect is not taken into account. Modifying the HF model (5) to include this effect, the new HF model is shown in (31).

$$\begin{bmatrix} v^r_{sdHF} \\ v^r_{sqHF} \end{bmatrix} = \begin{bmatrix} R_{dHF} & 0 \\ 0 & R_{qHF} \end{bmatrix} \begin{bmatrix} i^r_{sdHF} \\ i^r_{sqHF} \end{bmatrix} + p \begin{bmatrix} L_{dHF} & L_{qdHF} \\ L_{dqHF} & L_{qHF} \end{bmatrix} \begin{bmatrix} i^r_{sdHF} \\ i^r_{sqHF} \end{bmatrix} +$$
$$+ \begin{bmatrix} -\omega_r L_{dqHF} & -\omega_r L_{qHF} \\ \omega_r L_{dHF} & \omega_r L_{qdHF} \end{bmatrix} \begin{bmatrix} i^r_{sdHF} \\ i^r_{sqHF} \end{bmatrix} \quad (31)$$
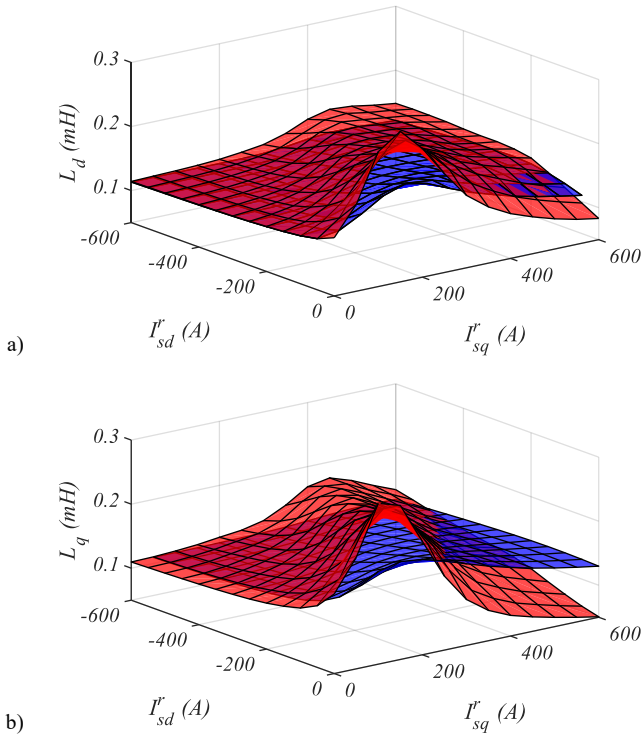
■ DC inductance ■ FEA HF inductance

a)

b)

Fig. 6 - a) *d*-axis HF and DC inductance vs. stator current and b) *q*-axis HF and DC inductance vs. stator current. I_{HF}=0.05 pu, ω_{HF}=2*π*500 rad/s, ω_r=500 rpm and T_r=20ºC.

Following the procedure described in Section III with the new HF model, the estimated HF inductances in (13) and (19) becomes (32) and (33), respectively. It is observed from (32) and (33) that actual d and q-axis HF inductances can be obtained by subtracting the cross-coupling (L_{qdHF} and L_{dqHF}) inductances

from estimated values. The cross-coupling inductances are defined in (34) and (35), being $L_{qdHF} = L_{dqHF}$.

$$\hat{L}_{dHF} = \Im[Z_{dHF}] / \omega_{HF} = L_{dHF} + L_{qdHF} \quad (32)$$

$$\hat{L}_{qHF} = \Im[Z_{qHF}] / \omega_{HF} = L_{qHF} + L_{dqHF} \quad (33)$$

$$L_{qdHF} = \frac{\partial \lambda_{sd}}{\partial i^r_{sq}} \quad (34)$$

$$L_{dqHF} = \frac{\partial \lambda_{sq}}{\partial i^r_{sd}} \quad (35)$$

In order to compensate for the cross-coupling inductance effect, cross-coupling inductance value must be known. It is possible to estimate the cross-coupling inductance using the q-axis stator flux response to the squarewave, small-amplitude, low frequency current signal already used in Section III. In Section III, only d-axis stator flux estimation from flux observer was used to estimate PM flux linkage; for cross-coupling inductance estimation, only q-axis stator flux estimation from flux observer will be used. The cross-coupling inductance is obtained in (36), being λ^{r+}_{sq} the q-axis flux linkage when positive d-axis current step, ΔI^r_{sd}, is applied, while λ^{r-}_{sq} is the q-axis flux linkage when negative d-axis current step, $-\Delta I^r_{sd}$, is applied.

$$L_{qdHF} = L_{dqHF} = \frac{\partial \lambda_{sq}}{\partial i^r_{sd}} \approx \frac{\Delta \lambda_{sq}}{\Delta i^r_{sd}} = \frac{\lambda^{r+}_{sq} - \lambda^{r-}_{sq}}{2\Delta I^r_{sd}} \quad (36)$$

B. DC inductance estimation from HF inductance

Another reason for the mismatch between estimated HF inductance and DC inductance is the magnetic saturation of the machine. While the DC inductance is defined as the linearized or apparent inductance from the origin to the operating point, the HF (or dynamic) inductance is defined as the variation of the flux respect the current (37) i.e. the slope of the flux-current curve around the operating point [27]. This is schematically shown in Fig. 7.

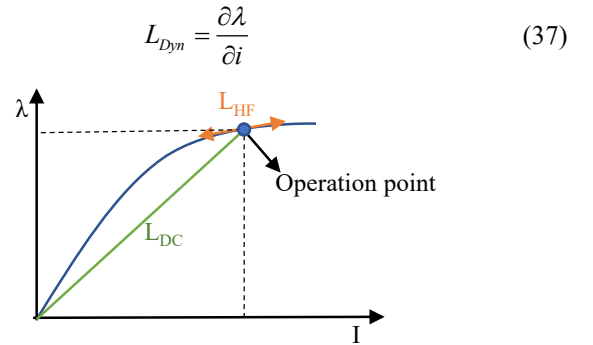$$L_{Dyn} = \frac{\partial \lambda}{\partial i} \quad (37)$$

Fig. 7 – Schematic representation of DC or linearized inductance and HF or incremental inductance.

In order to obtain the DC inductances from the HF results, the HF inductance can be integrated along the current trajectory of the machine. This technique will provide instantaneous DC

inductance estimation in d and q-axis using the estimated HF inductance, as shown in (38) and (39).

$$L_{dDC} = \frac{\int L_{dDyn}(I^r_{sd}, I^r_{sq})\partial i^r_{sd} - \lambda_{pm}(I^r_{sd}, I^r_{sq})}{I^r_{sd}} \quad (38)$$

$$L_{qDC} = \frac{\int L_{qDyn}(I^r_{sd}, I^r_{sq})\partial i^r_{sq}}{I^r_{sq}} \quad (39)$$

C. Simulation results

HF inductances are calculated using (32) and (33) to take into account the cross-coupling inductance. The cross-coupling inductance is obtained from (36) using the q-axis flux observer output estimation. Fig. 8a and 8b show the estimated d and q-axis HF inductances considering the cross-coupling inductance, respectively. For the sake of comparison, Fig. 8a and 8b, also show the dynamic inductances theoretically calculated from FEA data using (37) for both d and q-axis. It is observed that HF and dynamic inductances are matching as it was expected.


■ Dyn inductance   ■ FEA HF inductance
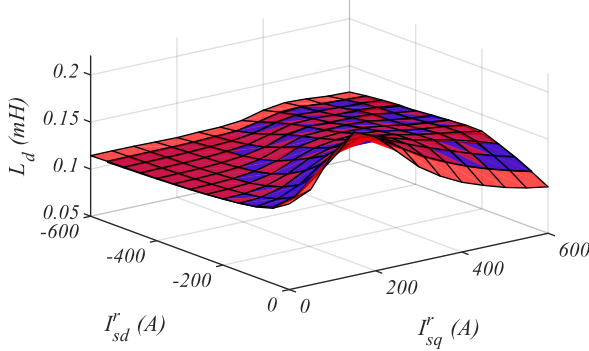
a)
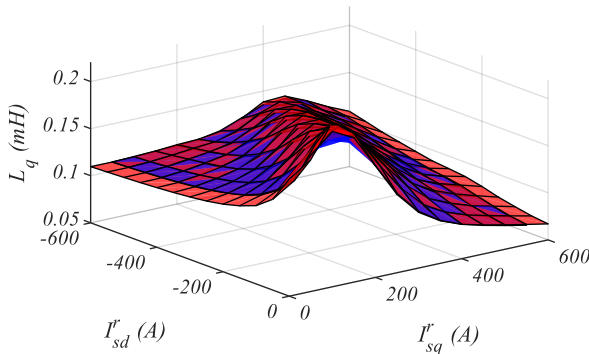
b)

Fig. 8 - a) d-axis HF and Dynamic inductance vs. stator current and b) q-axis HF and Dynamic inductance vs. stator current. I_{HF}=0.05 pu, ω_{HF}=2*π*500 rad/s, ω_r=500 rpm and T_r=20ºC.

In order to further enhance the stator flux observer estimation, instead of introducing the HF inductances into the flux observer, the DC inductance values are estimated using (38) and (39). Fig. 9a and 9b show the estimated d and q-axis DC inductances, respectively, and actual d and q-axis DC inductances are also shown for comparison. It is observed that estimated and actual DC inductances are matching as it was expected.

■ DC inductance   ■ FEA estimated DC inductance
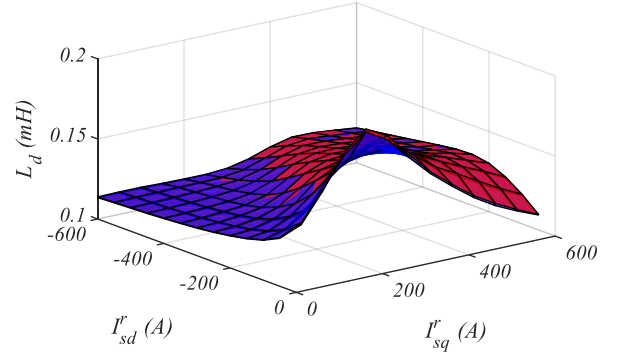
a)
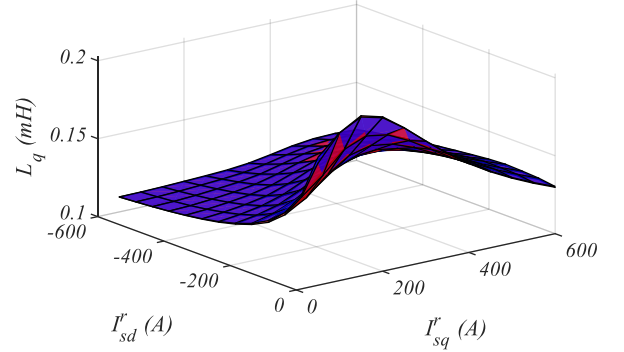
b)

Fig. 9 - a) d-axis estimated and actual DC inductance vs. stator current and b) q-axis estimated and actual DC inductance vs. stator current. I_{HF}=0.05 pu, ω_{HF}=2*π*500 rad/s, ω_r=500 rpm and T_r=20ºC.

After the stator inductances are estimated, using the procedure described in Section III, the stator resistance is estimated and represented in Fig. 2c.

The last parameter to be estimated is the PM flux linkage, it is estimated using a square-wave current signal with $\pm \Delta I^r_{sd}$=0, as described in Section III. Fig. 2d shows the estimated PM flux linkage using this procedure.

The estimated parameters and PM flux linkage are used in the Gopinath type flux observer. Estimated d and q-axis stator flux are shown in Fig. 10a and 10b, respectively, and actual machine flux from FEA data is also represented for comparison. The stator flux observer provides an accurate estimation as it was expected. Finally, the torque is estimated using (2) and it is represented vs. stator current in Fig. 11a and the estimation error is calculated as (40) and shown in Fig. 11b, being $\hat{T}$ the torque estimated by proposed method and T_{FEA} the actually produced torque extracted from FEA results. It is observed from Fig. 10 that the method provides good accuracy in the whole stator current region. The largest error is produced at high load and deep flux weakening current region, where the machine is not likely to be operated. Furthermore, the maximum error magnitude is around 1 Nm, which is 0.4% of rated torque.

$$error = \hat{T} - T_{FEA} \quad (40)$$

V. Conclusions

This paper proposes a torque estimation method for VLF-PMSMs based on the stator flux linkage. Stator flux linkage is estimated using a flux observer. d and q-axis inductances and stator resistance are estimated online from the response of the machine to a pulsating HF current signal which is injected on top of the fundamental excitation. PM flux linkage is estimated from the response to a low-frequency, low-magnitude square-wave current which is also injected on top of the fundamental excitation. Cross-coupling inductance effect is compensated and DC inductance is obtained from HF values and used in the stator flux observer. Accurate stator flux estimation is obtained from flux observer using estimated parameters, leading to accurate torque estimation. Simulation results have been provided to demonstrate the validity of the proposed technique.

References

[1] V. Ostovic, "Memory motors", IEEE Ind. Appl. Mag., 9(1): 52–61, Jan. 2003.

[2] T. Kato, M. Minowa, H. Hijikata, K. Akatsu, and R. D. Lorenz, "Design Methodology for Variable Leakage Flux IPM for Automobile Traction Drives", IEEE Trans. Ind. Appl., 51(5): 3811–3821, Sep. 2015.

[3] A. Athavale, T. Fukushige, T. Kato, C. Yu, and R. D. Lorenz, "Variable Leakage Flux IPMSMs for Reduced Losses Over a Driving Cycle While Maintaining Suitable Attributes for High-Frequency Injection-Based Rotor Position Self-Sensing", IEEE Trans. Ind. Appl., 52(1): 234–241, Jan. 2016.

[4] Jang-Mok Kim and Seung-Ki Sul, "Speed control of interior permanent magnet synchronous motor drive for the flux weakening operation", IEEE Trans. Ind. Appl., 33(1): 43–48, Jan. 1997.

[5] C. Lin, S. Liang, J. Chen, and X. Gao, "A Multi-Objective Optimal Torque Distribution Strategy for Four In-Wheel-Motor Drive Electric Vehicles", IEEE Access, 7: 64627–64640, 2019.

[6] D. O. Neacsu and K. Rajashekara, "Comparative analysis of torque-controlled IM drives with applications in electric and hybrid vehicles", IEEE Trans. Power Electron., 16(2): 240–247, Mar. 2001.

[7] Z. Zhang, R. Ma, L. Wang, and J. Zhang, "Novel PMSM Control for Anti-Lock Braking Considering Transmission Properties of the Electric Vehicle", IEEE Trans. Veh. Technol., 67(11): 10378–10386, Nov. 2018.

[8] P. Sue, D. Wilson, L. Farr, and A. Kretschmar, "High precision torque measurement on a rotating load coupling for power generation operations", in IEEE Int. Instrum. Meas. Technol. Conf. Proc., pp: 518–523, May 2012.

[9] K. C. Yeo, G. Heins, and F. De Boer, "Comparison of torque estimators for PMSM", in Australas. Univ. Power Eng. Conf., pp: 1–6, Dec. 2008.

[10] B. Cheng and T. R. Tesch, "Torque Feedforward Control Technique for Permanent-Magnet Synchronous Motors", IEEE Trans. Ind. Electron., 57(3): 969–974, Mar. 2010.

[11] M. Martinez, D. Reigosa, D. Fernández, J. M. Guerrero, and F. Briz, "PMSMs Torque Estimation Using Pulsating HF Current Injection", in 2018 IEEE 9th Int. Symp. Sensorless Control Electr. Drives SLED, pp: 96–101, Sep. 2018.

[12] F. Jukic, D. Sumina, and I. Erceg, "Comparison of torque estimation methods for interior permanent magnet wind power generator", in Int. Conf. Electr. Drives Power Electron. EDPE, pp: 291–296, Oct. 2017.

[13] J. X. Xu, S. K. Panda, Y. J. Pan, T. H. Lee, and B. H. Lam, "Improved PMSM pulsating torque minimization with iterative learning and sliding mode observer", in IEEE Int. Conf. Ind. Electron. Control Instrum., Nagoya, Japan, 3, pp: 1931–1936, 2000.
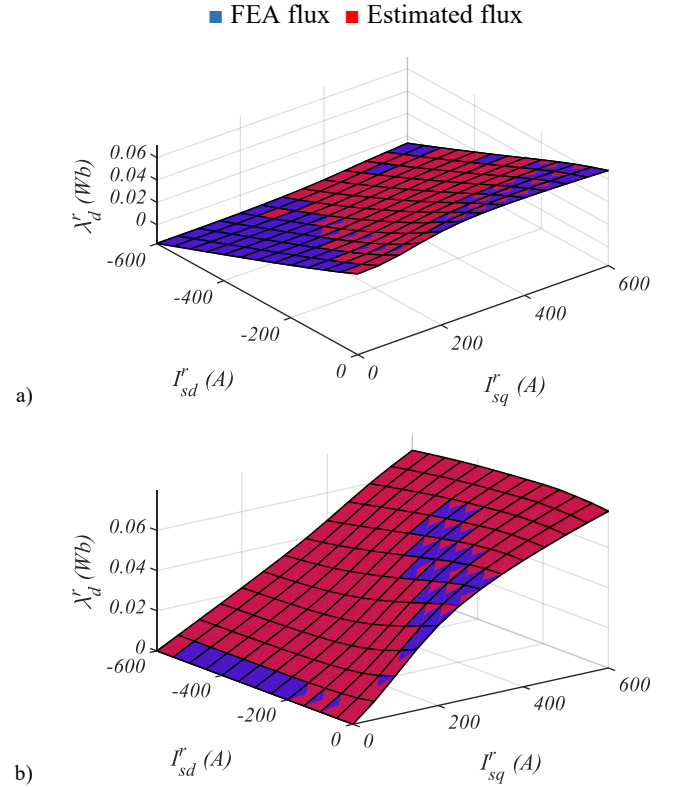
Fig. 10 - a) estimated and actual d-axis flux vs. stator current and b) estimated and actual q-axis flux vs. stator current. I_{HF}=0.05 pu, ω_{HF}=2*π*500 rad/s, ω_r=500 rpm and T_r=20ºC.
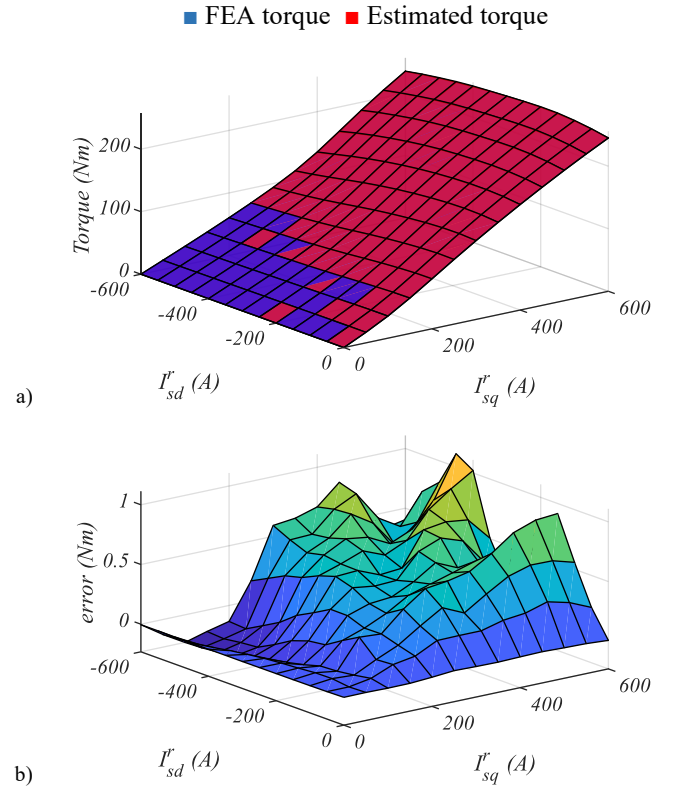

Fig. 11 - a) estimated and FEA output torque, and b) estimation error. I_{HF}=0.05 pu, ω_{HF}=2*π*500 rad/s, ω_r=500 rpm and T_r=20ºC.

[14] Weizhe Qian, S. K. Panda, and Jian-Xin Xu, "Torque ripple minimization in PM synchronous motors using iterative learning control", IEEE Trans. Power Electron., 19(2): 272–279, Mar. 2004.

[15] Se-Kyo Chung, Hyun-Soo Kim, Chang-Gyun Kim, and Myung-Joong Youn, "A new instantaneous torque control of PM synchronous motor for high-performance direct-drive applications", IEEE Trans. Power Electron., 13(3): 388–400, May 1998.

[16] X. Dong, W. Tianmiao, and W. Hongxing, "Comparison between model reference observer and reduced order observer of PMSM torque", in IEEE Conf. Ind. Electron. Appl., pp: 663–667, Jun. 2011.

[17] Q. Liu and K. Hameyer, "High-Performance Adaptive Torque Control for an IPMSM With Real-Time MTPA Operation", IEEE Trans. Energy Convers., 32(2): 571–581, Jun. 2017.

[18] Y. A.-R. I. Mohamed and T. K. Lee, "Adaptive self-tuning MTPA vector controller for IPMSM drive system", IEEE Trans. Energy Convers., 21(3): 636–644, Sep. 2006.

[19] W. F. Traoré and R. McCann, "Torque measurements in synchronous generators using giant magnetoresistive sensor arrays via the Maxwell stress tensor", in 2013 IEEE Power Energy Soc. Gen. Meet., pp: 1–5, Jul. 2013.

[20] Z. Lin, D. S. Reay, B. W. Williams, and X. He, "Online Modeling for Switched Reluctance Motors Using B-Spline Neural Networks", IEEE Trans. Ind. Electron., 54(6): 3317–3322, Dec. 2007.

[21] J. F. Gieras, Permanent magnet motor technology: design and applications. CRC press, 2009.

[22] H.-S. Jung, D. Park, H. Kim, S.-K. Sul, and D. J. Berry, "Non-Invasive Magnet Temperature Estimation of IPMSM Based on High-Frequency Inductance With a Pulsating High-Frequency Voltage Signal Injection", IEEE Trans. Ind. Appl., 55(3): 3076–3086, May 2019.

[23] D. Reigosa, D. Fernández, M. Martínez, J. M. Guerrero, A. B. Diez, and F. Briz, "Magnet Temperature Estimation in Permanent Magnet Synchronous Machines Using the High Frequency Inductance", IEEE Trans. Ind. Appl., 55(3): 2750–2757, May 2019.

[24] J. S. Lee, C.-H. Choi, J.-K. Seok, and R. D. Lorenz, "Deadbeat-Direct Torque and Flux Control of Interior Permanent Magnet Synchronous Machines With Discrete Time Stator Current and Stator Flux Linkage Observer", IEEE Trans. Ind. Appl., 47(4): 1749–1758, Jul. 2011.

[25] P. L. Jansen and R. D. Lorenz, "A physically insightful approach to the design and accuracy assessment of flux observers for field oriented induction machine drives", IEEE Trans. Ind. Appl., 30(1): 101–110, Jan. 1994.

[26] T. Kato, T. Matsuura, K. Sasaki, and T. Tanimoto, "Principle of variable leakage flux IPMSM using arc-shaped magnet considering variable motor parameter characteristics depending on load current", in Proc IEEE Energy Convers Congr Expo, pp: 5803–5810, Oct. 2017.

[27] W. Xu and R. D. Lorenz, "High-Frequency Injection-Based Stator Flux Linkage and Torque Estimation for DB-DTFC Implementation on IPMSMs Considering Cross-Saturation Effects," IEEE Trans. Ind. Appl., 50(6): 3805-3815, Nov.-Dec. 2014.